Thin Films of Polyethylenimine and Alkyltrimethylammonium Bromides at the Air/Water Interface

Benjamin M. D. O'Driscoll, Elizabeth Milsom, Cristina Fernandez-Martin, Lyndsey White, Stephen J. Roser, and Karen J. Edler*

Department of Chemistry, University of Bath, Bath, Avon, UK BA2 7AY

Received March 6, 2005; Revised Manuscript Received August 1, 2005

ABSTRACT: We have prepared and analyzed thin film structures formed by polyethylenimine and alkyltrimethylammonium bromide (C_nTAB) surfactants at the air/water interface, using both surface and bulk sensitive techniques. In initial experiments it was observed that hexagonal arrays of rodlike micelles surrounded by the polymer were formed at the solution surface, with the principal axis of the micelles running parallel to the surface. In the studies reported here, the formation of these ordered mesostructured films was identified as being kinetically but not thermodynamically favored, with some of the systems examined showing a loss of structure from their neutron reflectometry profiles with time. The polymer was used in both an as-diluted state (with a small net positive charge) and a neutral state, through the addition of sodium hydroxide to the solution. The primary interaction in these systems was found to be that of a neutral polymer with a cationic surfactant; however, by modifying the charge on the polymer it is possible to alter the distance between micelles by up to 6 Å without destroying the structure of the films. Analysis of the bulk solution with small-angle neutron scattering showed that the micelles in solution are elliptical rather than rod-shaped, and so the assembly of the hexagonal mesostructure occurs at the air/water interface rather than adsorbing to the interface from the bulk.

Introduction

Mixed polyelectrolyte/surfactant systems are of interest because the interactions of the two components can lead to significant changes to the properties of the pure materials, such as the formation of aggregates below the critical micelle concentration (cmc). Understanding these changes is important for many commercial systems where polyelectrolytes and surfactants are combined, for instance in cosmetics, detergents, paints, foods,[1] and biotechnological applications such as DNA transfection.[2] Polyelectrolyte−surfactant interactions have been examined extensively in bulk phases, both solids and liquids, and these have been reviewed.[3−5] Recently, however, increasing interest has been shown in the surface properties of water-soluble polymer/surfactant solutions.[6] These studies have usually focused on either neutral polymers with ionic surfactants[7−9] or charged polymers with oppositely charged surfactants.[10−15] The behavior of the mixed system is highly dependent on the characteristics of both the polymer (including charge density,[16,17] MW,[18] and hydrophobicity[19]) and surfactant (including concentration and charge[18]). Some work has also been carried out on interactions between polyelectrolytes and surfactants with similar charges.[19−21] These can also form complexes in solution due to hydrophobic interactions and hydrogen bonding.

Polymer films on supports may be prepared a number of ways, including spin or dip coating of substrates[22] and, in the case of chargeable polymers, by using layer-by-layer deposition.[23,24] Complexes of similarly charged polymers and surfactants at the air−solution interface have been prepared by spreading of a Langmuir monolayer of a surfactant on a solution of polyelectrolytes.[21] However, these films are not solid and were not able to be transferred to a substrate by Langmuir−Blodgett techniques. It is rare for a water-soluble polymer to spontaneously self-assemble into large-scale structures at the air/water interface. In a previous communication[25] we reported the formation of solid mesostructured films of the branched polymer polyethylenimine (PEI: $[CH_2CH_2NH]_n$) and C_{16}TAB at the air/water interface which are easily visible to the naked eye. In the pH range used for these experiments (between 10 and 13) PEI has a small net positive charge, and the formation of micron thick films seemed to indicate that it was possible to have large-scale aggregates of like-charged surfactants and polymers. In the literature only a few reports examine systems containing PEI and C_nTAB.[26−29] In these studies an interaction between the polymer and surfactant was observed (manifested as a change in the pK_a of PEI and a shift of the cmc of C_{16}TAB to higher concentrations); however, no large-scale structures at the air/water interface were reported.

In the case of oppositely charged surfactants and polyelectrolytes a paper published since our initial report has also reported the formation of an ordered liquid crystalline phase in a polymer−surfactant layer at the air−water interface. In this case a 2 wt % solution of poly(diallyldimethylammonium chloride) and 10^{-4} M sodium dodecyl sulfate (SDS) formed an interfacial complex about 23 Å thick. Addition of 0.1 M NaCl to this solution resulted in "crystallization" of this film into a hexagonal phase composed of close-packed cylindrical micelles aligned parallel to the interface, similar to our PEI−C_nTAB films. The formation of the ordered liquid crystalline structure was suggested to be due to charge screening of the surfactant after the addition of salt, allowing initially spherical micelles to become cylindrical, followed by enhanced polyelectrolyte binding to the micelles due to the favorable entropic mechanism of counterion release.

* Corresponding author: Tel +44 1225 384192; e-mail K.Edler@bath.ac.uk.

10.1021/ma050469k CCC: $30.25
Published on Web 09/15/2005

Interfacial microgels formed from C_{12}TAB and poly(styrenesulfonate) have also been reported to form at the air−solution interface, but these are liquid films, which lower the surface tension at the solution−air interface. These films can be observed after drainage to form a suspended foam film although the details of the nanoscale structure were not measured.[12,30] Thin layers of DNA complexed with C_{12}TAB at the air−water interface have also more recently been reported. These were prepared with short DNA fragments (around 50 nm) in 20 mM NaBr, conditions where the DNA was only effectively 20% charged due to counterion condensation. The film formed at the point where surfactant−DNA binding in the bulk was saturated, just above the critical aggregation concentration (cac) and before the formation of precipitate, when the film thickness decreased. Brewster angle micrographs showed that the film was solidlike and could be cracked. The structure was suggested to be hexagonal since, at the cac, hexagonal composites of the DNA and surfactant have been observed in the bulk solution, although no measurements were made on the film.[31]

In this paper we report in greater detail factors affecting the formation of solid films of polyethylenimine−C_{16}TAB at the air solution interface. We also report films prepared with the shorter chained surfactants tetradecyltrimethylammonium bromide (C_{14}TAB) and dodecyltrimethylammonium bromide (C_{12}TAB). We have investigated the effect of surfactant chain length on the macroscale and mesoscale structures and formation mechanisms of these films. The mixed polymer/surfactant solutions were examined primarily with small-angle neutron scattering (SANS) and neutron reflectometry to determine the state of the systems in the bulk and at the air/water interface. Examination of the films was also performed with Brewster angle microscopy (BAM), surface pressure measurements, and visual observation of the growth of the films.

Experimental Section

Branched PEI (MW ≈ 750 000, 2000 Da) as 50% weight solutions, sodium hydroxide, hydrochloric acid, hydrobromic acid, and C_{14}TAB were purchased from Sigma-Aldrich, and C_{12}TAB and C_{16}TAB were purchased from Acros Organics. All the chemicals were used without further purification. Ultrapure Milli-Q water (18.2 MΩ cm resistance) was used as the solvent.

To simplify the analysis of the data, the PEI concentration is measured relative to a standard concentration of polymer (60 g/L ≈ 1.393 mol of monomeric unit/L); this concentration is referred to as a conc 1 solution. The terms long and short PEI are also used when referring to solutions of the 750 000 and 2000 Da MW polymers, respectively.

For the majority of the BAM, neutron reflectometry, and surface pressure measurements a solution of C_nTAB was added to a solution containing the PEI in a volume-to-volume basis. However, for the neutron reflectometry experiments on the C_{16}TAB/PEI system and the SANS experiments a weight-to-weight addition was used; this results in a maximum error (for the conc 1 solutions) of 3% in the PEI concentration due to the density of the PEI solution. This was not considered significant as there is a twofold difference in adjacent PEI concentrations, and therefore no distinction was made between the weight-to-weight and volume-to-volume solutions.

The concentration of the surfactant was set at a value of 0.037 M, except for the experiments examining the film formation times where it was necessary to alter both the surfactant and polymer concentrations. This concentration is above the cmc (spherical micelles) for the surfactants used but below the sphere−rod phase transition point. Comparing the concentration of monomeric units of the polymer to the concentration of the surfactant gives a ratio of ∼37.7 PEI monomers/C_nTAB molecule in a conc 1 solution.

For the neutron reflectometry experiments the PEI/C_nTAB solutions were placed in Teflon troughs, 152 × 42 mm, which hold 20−30 mL of liquid. For the surface tension, film formation, and BAM experiments circular polystyrene dishes, 62 mm in diameter, containing 20 mL of solution were used.

The neutron reflectometry and SANS profiles were collected on the SURF,[32] CRISP,[33] and LOQ[34] instruments, at the ISIS Pulsed Neutron and Muon source, Rutherford Appleton Laboratories, Chilton, England. The incident angle used for the reflectometry experiments was 1.5°, with data being collected between 0.048 and 0.613 Å^{-1} in Q_Z ($= 4\pi \sin \theta_Z/\lambda$) on D_2O at room temperature. To determine any changes in the reflectometry profile with time, two or more measurements were performed on each film. These were timed from when the PEI and C_nTAB solutions were mixed, with generally one measurement being taken between 0 and 15 min and a second from 15 to 30−60 min depending on the quality of the data. If significant changes were occurring, then a third measurement was begun at the 30 min mark. Some experiments using D_{29}-C_{14}TAB and D_{25}-C_{12}TAB (purchased from CDN Isotopes) on air-contrast-matched water were also performed to determine the effect that replacing water with D_2O had on the structures formed at the air/water interface. Where possible, the reflectometry profiles were modeled with the Parratt program (Hahn-Meitner Institute).[35] SANS data were collected using two contrasts, 100% D_2O with protonated polymer and surfactant and 40%/60% D_2O/water with deuterated surfactant, from 0.09 to 0.285 Å^{-1} in Q_Z for 20 min at 25 °C. This temperature is close to the Krafft temperature for C_{16}TAB; however, the solutions remained clear at all times, and no evidence of crystallization was observed, suggesting the Krafft temperature for the mixed PEI−C_{16}TAB system is below 25 °C. SANS on C_{14}TAB solutions gave substantially similar results to those from the C_{16}TAB system despite the lower Krafft temperature for this surfactant. A background consisting of 0.2 M HCl in the appropriate D_2O/water mixture was subtracted, and the data were reduced to one dimension by radial averaging using the Collette program on LOQ. The patterns taken at different D_2O/water contrasts were modeled simultaneously using a procedure written by Dr. Steve Klein at the NIST Centre for Neutron Scattering for the Igor PRO platform (WaveMetrics). This procedure utilizes a least-squares fitting method that models multiple data sets as a uniform ellipsoid for the shape of the micelles in the solution. The two most significant parameters in determining the micellar shape are the micelle width and the micelle length, where the shape is given by width × width × length. Interactions between micelles were accounted for using a Hayter−Penfold[36] formalism for describing interactions between charged micelles in solution.

Surface tension measurements were performed with a tensiometer (Nima Technologies) and either paper or aluminum foil Wilhelmy plates. As no solvent-only zero point could be determined for these systems, the surface tension was zeroed with the Wilhelmy plate (wet in the case of paper plates) out of the solution, with the plate being dipped into the solution after the mixing (zero time) of the polymer and surfactant. In interpreting the data from these measurements, the properties of the films need to be considered, in particular the thickness and gellike nature of the films. These features may significantly interfere with the way the films interact with the Wilhelmy plates, and so the surface tension data can only be considered in a qualitative sense.

Three films, C_{16}TAB with long PEI conc 1, 1/2, and 1/4, were transferred to solid supports by placing a glass slide of known weight into the bottom of a PTFE trough prior to transferral of the surfactant−polymer solution and then lifting the slide out after 30 min. Care was taken to minimize the disruption of the film during transferral, and the bottom of the slide was wiped dry prior to weighing of the slide + film. The film was then dried in an oven at 100 °C for 2 periods of 1 h each, with the film being weighed at the end of each period. A single film

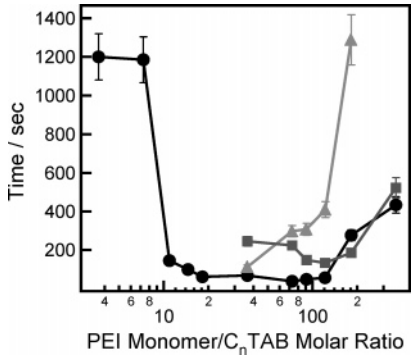

Figure 1. Visually observed film formation times for long PEI with C_{16}TAB (black circles), C_{14}TAB (dark gray squares), and C_{12}TAB (light gray triangles).

was also transferred from a C_{16}TAB with long PEI conc 1 using a 24 mm wide platinum/iridium ring, and a similar drying procedure was used. For all four films there was no significant difference between the weights measured at the end of each drying period.

The BAM images were collected using a NFT Nanoscope2 Brewster angle microscope.

Results

Film Formation. As has been previously reported,[25] the mixing of solutions of PEI and C_nTAB results in the formation of micron thick films at the air/water interface, which can be easily seen with the naked eye. For the short PEI systems, the films refract light to produce a distinct rainbow pattern at the interface, and this allows fault lines to be seen in the films. Generally, the size of coherent PEI/C_nTAB islands was on the order of 10 mm in diameter. For the long PEI systems the films were much thicker, up to about 100 μm thick, and a few minutes after the mixing of the PEI and C_nTAB the film is more accurately described as a skin rather than a thin film. This skin was resistant to puncture (though sticky) and wrinkled when the subphase below it was agitated. Puncturing it with a Pasteur pipet resulted in tearing of the films forming sharp edges which remained sharply defined over many minutes. Although film eventually re-forms where the solution surface is exposed, the sharp edges of the break remain visible in the film surface, indicating that the film is solid after it has formed.

Visual observation of these characteristic features of film formation can be used to determine the time taken for the films to form. By varying either the polymer or surfactant concentration, a wide range of polymer/surfactant ratios were examined (Figure 1). Identification of a point defining film formation is rather subjective, but repeated measurements by a single observer give consistent results within the error bars shown. For the long PEI and C_{16}TAB system there is a U-shaped dependence in the formation times, with the minimum time occurring between the ratios of 10 and 125 monomeric units of polymer per molecule of surfactant. Small variations in the time taken for film formation occur when the surfactant chain length is shortened, the most obvious of which is a sharp rise in the time taken for film formation at high monomer/surfactant ratios (>125) for C_{12}TAB. When the ratio of monomer/surfactant becomes very high (>450), no film formation is observed.

After long periods of time, for example 42 h for C_{14}TAB with conc 1/2 long PEI, the wrinkling behavior of the long PEI films was found to disappear, though prodding the surface with a spatula showed that a film was still present. Another feature of these films is the necessity of an open atmosphere above the solution. If the mixed PEI/C_nTAB solution is stored in a closed vial, no film will form at the interface, and if the dish in which a film has already formed is covered, then the film will dissolve from the surface. It is therefore likely that evaporation from the surface is important to the formation of the films.

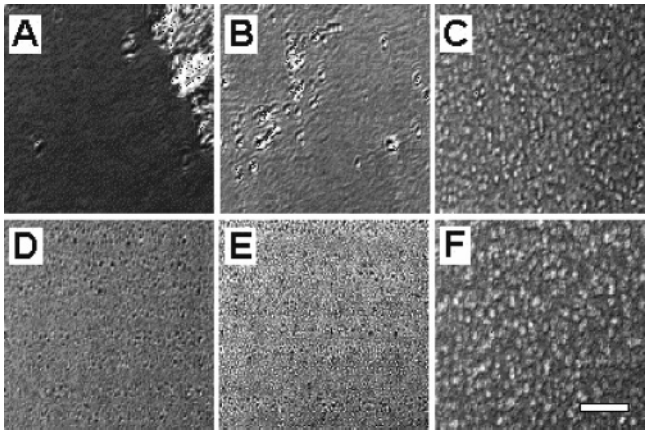

Figure 2. Selected BAM images of PEI/C_nTAB films taken 30 min after the mixing of the reactant solutions: (A) C_{16}TAB long PEI conc 1, (B) C_{14}TAB long PEI conc 1, (C) C_{14}TAB long PEI conc 1/16, (D) C_{14}TAB short PEI conc 1, (E) C_{12}TAB short PEI conc 1, and (F) C_{12}TAB short PEI conc 1/16. Scale bar = 50 μm.

Using the weight of the C_{16}TAB long PEI conc 1 film transferred to a glass slide and approximating the density of the film as 0.98 g/mL, it was calculated that thickness of the film formed was ~92 μm. For the conc 1/2 and conc 1/4 films the thickness decreased to 59 and 52 μm, respectively. Upon drying of the films there is a significant loss of weight, such that the dry weight of the films was 11%, 8%, and 6% of the wet weight for the conc 1, 1/2, and 1/4 films, respectively. It is possible that some of subphase may have been trapped under the film when it was transferred onto the glass slide. This is supported by the results for film transferred using the Pt/Ir ring, which had a dry weight that was 18% of the wet weight; however, for this film the amount of film transferred per unit area was only 69% percent of that transferred using the glass slide. It seems likely therefore that some of the subphase was transferred when a glass slide was used, while some of the film was left behind when the Pt/Ir ring was used.

By approximating the volume and density of a fully condensed PEI/C_{16}TAB film, it was calculated that the maximum thickness of the film could be no more than 5 μm given the dry weight of the films. The as-transferred (wet) film does not therefore consist entirely of a condensed polymer/surfactant mesostructure; this will be explored further in the discussion.

BAM. BAM images of the films were collected 5, 10, 20, and 30 min after the mixing of the polymer and surfactant for all three surfactants studied, at PEI concentrations of 1, 1/2, 1/4, 1/8, and 1/16 and for both long and short PEI (Figure 2 and Supporting Information). Consistent with the observations reported in the previous section, it was found that the mobility of the films (i.e., the speed at which individual features pass across the imaging area) in the short PEI systems was much higher than in the long PEI systems. However,

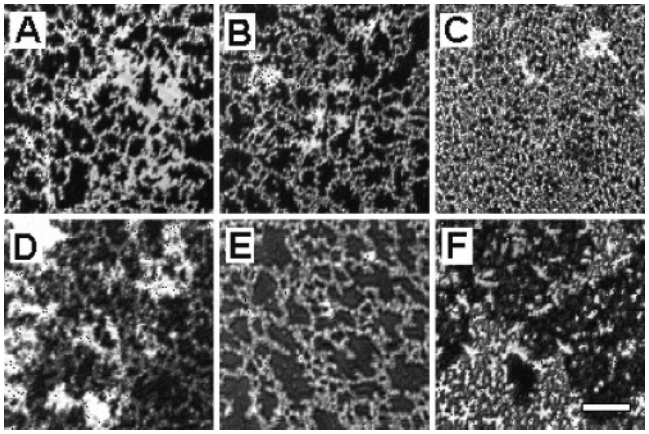

Figure 3. BAM images of C_{16}TAB short PEI conc 1: (A) 5, (B) 10, and (C) 30 min after mixing; (D) C_{16}TAB short PEI conc 1/2 5 min after mixing, (E) C_{14}TAB short PEI conc 1/2 5 min after mixing, and (F) C_{16}TAB short PEI conc 1 with 0.05 M NaOH 30 min after mixing. Scale bar = 50 μm.

the mobility of both the short and long PEI films decreased to near zero as the time after mixing increased, indicating the formation of more continuous, and therefore less mobile, films.

One of the more unusual features observed in the BAM images was a fractal-like growth pattern in the C_{16}TAB conc 1 and 1/2 and C_{14}TAB conc 1/2 short PEI films (Figure 3). For these films growth is achieved through the formation, lengthening, branching, and fusing of condensed areas of the film rather than the gradual condensing of the whole surface area as is observed in the majority of the BAM images.

When 0.05 M NaOH was added to C_{16}TAB short PEI conc 1, there was initially no difference between that film and the film without NaOH. However, after 20 min the fractal pattern was swamped by large nonfractal structures that appear to grow beneath the fractal structures (Figure 3f).

A series of BAM images taken of a film that was grown (exposed to an open/ unsaturated atmosphere), covered to dissolve the film (liquid−vapor equilibrium established), and then regrown showed that the structure of the film was unchanged during the two growth periods (Supporting Information). This behavior is only likely to occur if there is a complete breakup of the film upon the establishment of the liquid−vapor equilibrium.

Effect of pH on Film Formation. To determine the degree of amine protonation in the polymer, both long and short PEI were titrated against concentrated hydrochloric acid (Supporting Information). From these curves pK_a values (not corrected for ionic strength) for long (9.28) and short (9.56) were obtained. These values are higher than has been reported elsewhere;[37] however, variations in the structure of the polymer will affect the pK_a of the polymer significantly.

The most probable cause of this difference in the pK_a values for long and short PEI is the level of branching present in the two polymers. In simple amines, the acid/base dissociation constants for primary, secondary, and tertiary amines are different, with the secondary amines having the highest pK_a values of the three. Given that in the branching of the polymer chain a primary and a tertiary amine will form from the reaction of the monomer with a secondary amine, it is therefore likely that there is more branching in the higher MW polymer.

The pHs of both long and short PEI/C_{16}TAB solutions were also measured, and from these values the percentage of protonated amine groups for each polymer was determined to be 3% on average. The change in the pH was not however constant with increasing concentration; instead, the percentage of charge on the polymer decreased with increasing polymer concentration.

For long PEI with C_nTAB the measured pHs were slightly higher than those of pure long PEI, and so the interaction of the polymer and surfactant does influence the pH for long PEI. However, for short PEI there is no significant change in the pH relative to the pure solution. This difference may be attributed to the variation in the level of branching in the polymer and/or the thickness of the films. For long PEI systems the film, due to its substantial thickness, incorporates a sizable portion of the PEI present in the solution. For C_{16}TAB micelles it has been observed[38,39] that ~30% of the bromide counterions are not directly bound to the micelle. Consequently, if a second chargeable species (such as PEI) is present in the solution, it is probable that some of these bromide ions will associate with this second component, thereby stabilizing the charge on this second species. Along with these bromide-neutralized ammonium groups in the case of PEI there will be a number of charged groups that are neutralized by the hydroxyl ion generated when a hydrogen atom was taken up by the amine. Unlike the bromide ions, however, these hydroxyl ions are not considered to be closely bound to the cations due to their large hydration spheres. This has an impact on their incorporation into the film. The presence of a large number of hydrophobic moieties and the location of the film at the air/water interface will favor the incorporation of bromide ions over hydroxyl ions as the counterion in the film. In the case of long PEI, where a significant portion of the polymer is present in the film, this higher percentage of hydroxyl ions in the subphase relative to the film will lead to an increase in the pH of the solution, as was observed.

No film was formed when the percentage of charge ammonium groups was adjusted to >50% of the total number of amines, by changing the pH of the system to ~9 using hydrobromic acid. This is in line with the lack of interaction found in systems containing $C_{16}TA^+$ cation and the cationic polymer poly-L-lysine hydrobromide.[40] Conversely, as was previously reported,[25] the addition of sodium hydroxide to the polymer solution leads to an apparent increase in the film thickness. When 0.1 M NaOH was added to a pure PEI solution, the pH of the solution was found to be 12.92, giving a percentage of charged groups of 0.04%.

Surface Pressure. Surface pressure measurements on the PEI/C_nTAB films showed quite different behavior for long and short PEI. The films prepared using short PEI exhibit little or no change in the surface pressure over time, whereas the long PEI films show both strong temporal and concentration effects. The graphs of the long PEI and C_nTAB films are shown in Figure 4.

The most significant change in the equilibrium surface pressure is observed in the conc 1 films, with the equilibrium surface pressure generally decreasing as the concentration of the polymer is decreased. Exceptions to this pattern (such as the relatively high equilibrium surface pressure for the C_{12}TAB conc 1/16 film) were not considered significant for reasons outlined in the Experimental Section. The shapes of the curves reported in Figure 4 indicate that there are two or more processes occurring in the films at the air/water interface. The

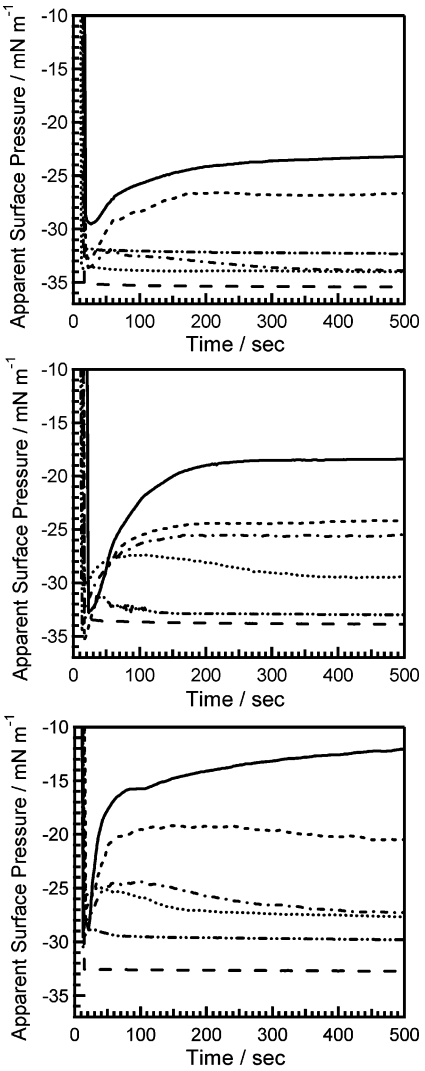

Figure 4. Apparent surface pressure vs time graphs for (top to bottom) C_{12}TAB, C_{14}TAB, and C_{16}TAB with long PEI at various PEI concentrations: conc 1 (—), conc 1/2 (- — -), conc 1/4 (- • — •), conc 1/8 (• • •), conc 1/16 (- • • -), and without PEI (- -).

first (excluding the initial sharp drop from the immersion of the Wilhelmy plate) is fast, dominating the curves up to the 200 s mark, and leads to an increase in the surface pressure in most of the curves. The second, and possibly third, process(es) are slow and have varied effects depending on the concentration of the polymer. The first process is sensitive to both the polymer concentration (decreasing as the concentration of polymer decreases) and the surfactant chain length (increasing both in rate and magnitude of change as the length of the alkyl chain increases). This chain length effect is most evident in the higher concentration films, with those with lower concentrations showing very similar behavior. The rate of this first process correlates well with the times reported in Figure 1, suggesting that this corresponds to the formation of, at the least, the upper most portions of the film. After the 200 s the conc 1 films exhibit a steady increase in the surface pressure, while for the conc 1/8 and 1/16 films there is a decrease in the surface pressure. It is possible that different processes dominate in these films.

SANS. SANS carried out on the PEI/C_nTAB systems and modeled with an ellipsoid model give quite varied micellar shapes (Supporting Information). In the C_{16}-TAB and C_{14}TAB long PEI systems the micelles are prolate ellipsoids, which elongate further as the concentration of PEI increases (Figure 5), though the lengths of the micelles reported here are less (by ~40 Å) than has previously been reported for a C_{16}TAB/PEI system.[28] For the C_{12}TAB and C_{14}TAB short PEI systems no trend was observed in the micellar shapes. In these systems modeling of the SANS profiles gave shapes ranging from disk-shaped (oblate ellipsoid) micelles (C_{14}TAB short PEI conc 1/4 and C_{12}TAB long PEI conc 1, 1/2, 3/4, and 1/4) to spherical micelles (C_{14}TAB short PEI conc 1/2 and 1/8 and C_{12}TAB long PEI conc 1/8) to prolate ellipsoid micelles with no obvious trend from one shape to another.

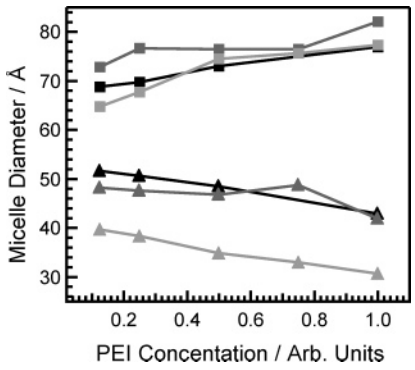

Figure 5. Plots of the total micelle width (triangles) and length (squares) for C_{16}TAB with long PEI (black), C_{16}TAB short PEI (dark gray), and C_{14}TAB long PEI (light gray).

The presence of elliptical micelles is consistent with the results reported by Berr et al. on pure C_nTAB micelles in D_2O and 50% D_2O,[41] though generally the micelle shapes reported here are more elongated and have smaller widths. This change, along with the trend toward greater elongation with increasing PEI concentration, points to an interaction between the surfactant micelles and the polymer. This interaction is greatest in the C_{16}TAB/PEI systems.

Neutron Reflectometry. The neutron reflectometry profiles for the two polymers and three surfactants are given in Figure 6. All the scans shown are the final or "equilibrium" scan collected for each film and so give the structure of the films 15+ min after the mixing of the polymer and surfactant solutions.

For the six PEI/C_nTAB systems examined Bragg diffraction, resulting from the self-assembly of ordered structures at the interface, is present in some or all of the films. Previously, we identified this structure using grazing incidence X-ray diffraction (GIXD) (for a C_{16}-TAB conc 1 short PEI with 0.1 M NaOH) as corresponding to a hexagonal array of rodlike micelles with the long axis of the micelle orientated parallel to the air/water interface. Given the similarities of the systems being examined here, it is likely that a similar arrangement is responsible for the diffraction peaks visible in the reflectometry profiles of these films. However, on these data alone we cannot rule out the formation of lamellar phases in the films, which would give similar profiles. As expected for either structure, the spacing between adjacent repeat units (i.e., the centers of adjacent cylinders in the case of the hexagonal structure) decreases as the length of the surfactant alkyl chain decreases (Table 1). Within each system there is also a general increase in the spacing between repeat units as the concentration of PEI decreases.

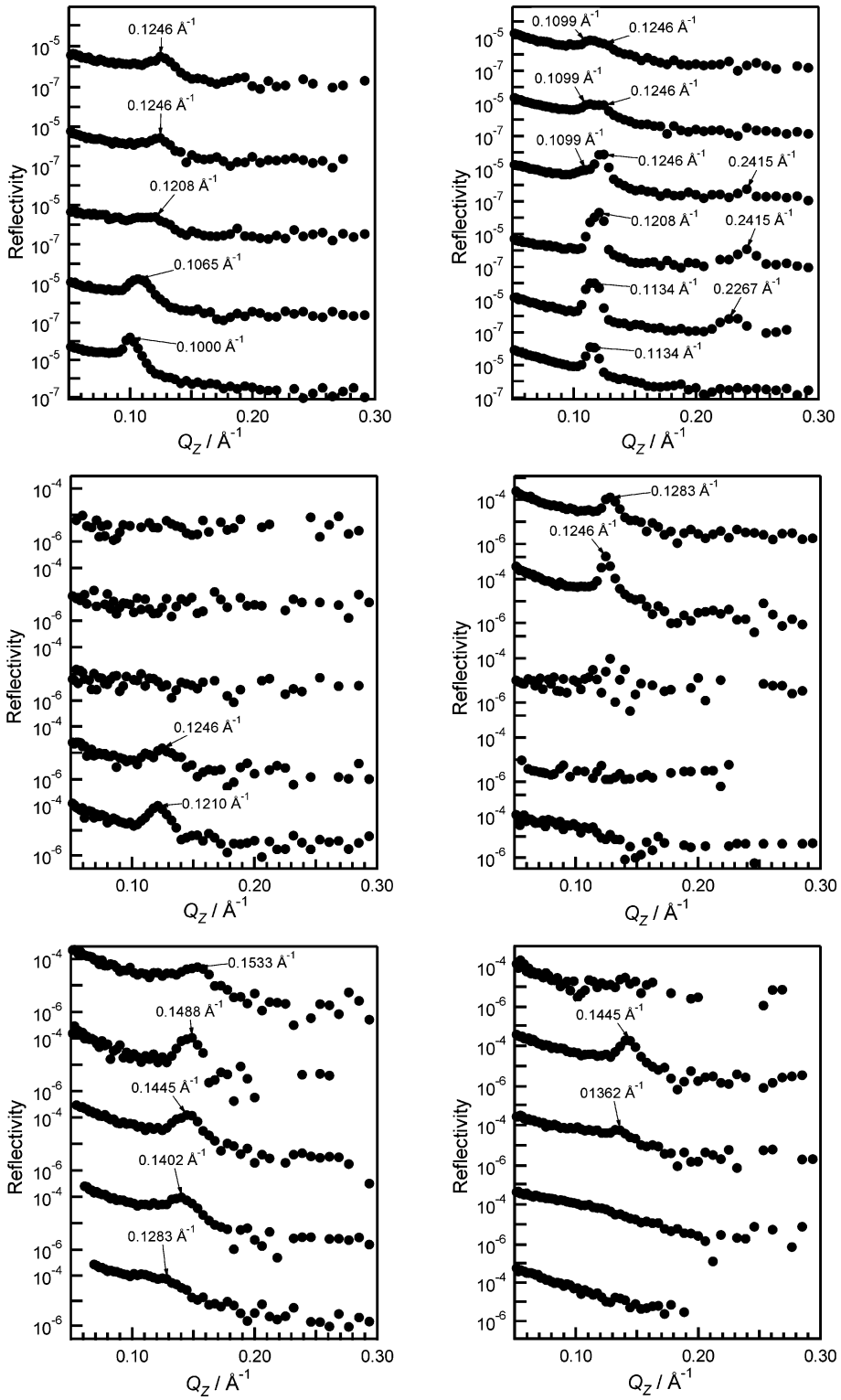

Figure 6. (a) Neutron reflectometry profiles, with peak positions indicated, for C_{16}TAB with long and short PEI. Top to bottom: long PEI: conc 1/2, 1/4, 1/8, 1/16, and 1/32; short PEI: conc 1, 3/4, 1/2, 1/8, 1/16, and 1/32. (b) Neutron reflectometry profiles, with peak positions indicated, for C_{14}TAB with long and short PEI. Top to bottom: long PEI: conc 1, 1/2, 1/4, 1/8, and 1/16; short PEI: conc 1, 1/2, 1/4, 1/8, and 1/16. (c) Neutron reflectometry profiles, with peak positions indicated, for C_{12}TAB with long and short PEI. Top to bottom: long PEI: conc 1, 1/2, 1/4, 1/8, and 1/16; short PEI: conc 1, 1/2, 1/4, 1/8, and 1/16.

For the PEI/C_nTAB systems all of the observed spacings are greater than both the width of the micelles that we calculated from the SANS patterns and the diameter of rod-shaped C_nTAB micelles in solution; for pure C_{16}TAB values of 45.0 and 46.6 Å have been reported for the rod width,[42,43] for C_{14}TAB this width decreased to 43.6 Å in 0.020 M NaBr,[44] and for C_{12}TAB (as a 15% mix with sodium dodecyl sulfate) the rod width was 34 Å.[45] The size of the spacings observed here can therefore only be attributed to PEI intercalated between the C_nTAB micelles.

Despite the fact that the majority of the systems examined displayed Bragg diffraction, some of the films also exhibited a decrease in the diffraction intensity with time. This decrease was most dramatic in the films prepared using short PEI, where, in a number of the

Table 1. Peak Positions and Distances between Adjacent Repeat Units for the Films in Which Bragg Diffraction Is Observed[a]

C_{12}TAB	Q_Z (Å^{-1})	distance (Å)
S-conc 1/2	0.1445	50.23
S-conc 1/4	0.1362	53.28
L-conc 1	0.1533	47.34
L-conc 1/2	0.1488	48.76
L-conc 1/4	0.1445	50.23
L-conc 1/8	0.1402	51.73
L-conc 1/16	0.1283	56.53
C_{14}TAB	Q_Z (Å^{-1})	distance (Å)
S-conc 1	0.1283	56.53
S-conc 1/2	0.1246	58.22
S-conc 1/4	0.1283	56.53
L-conc 1/8	0.1246	58.22
L-conc 1/16	0.1210	59.97
C_{16}TAB	Q_Z (Å^{-1})	distance (Å)
S-conc 1	0.1099, 0.1246	66.16, 58.22
S-conc 3/4	0.1099, 0.1246	66.16, 58.22
S-conc 1/2	0.1099, 0.1246	66.16, 58.22
S-conc 1/8	0.1208	60.08
S-conc 1/16	0.1134	63.99
S-conc 1/32	0.1134	63.99
L-conc 1/2	0.1246	58.22
L-conc 1/4	0.1246	58.22
L-conc 1/8	0.1208	60.08
L-conc 1/16	0.1065	68.16
L-conc 1/32	0.1000	72.58

[a] *S* and *L* refer to short and long PEI, respectively. There is an error of 1.6% associated with each of these values.

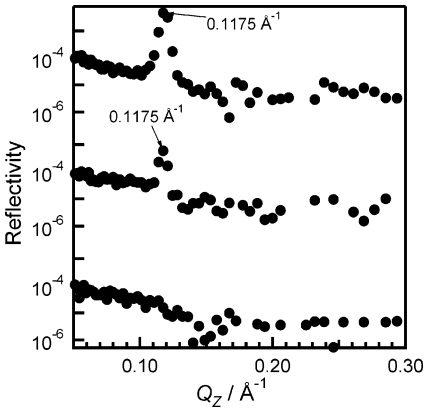

Figure 7. Neutron reflectometry profiles of C_{14}TAB short PEI conc 1/16. Top to bottom: film formation up to 15 min, between 15 and 30 min, and over 30 min after mixing.

systems studied (C_{12}TAB conc 1, 1/8, and 1/16 and C_{14}-TAB 1/4, 1/8, and 1/16), no distinct diffraction peak could be seen in the final pattern (Figure 7). Modeling of the neutron reflectometry profiles of these films confirms that there is little or no order present at the interface—although the scattering length densities calculated for the "bulk" are significantly lower than pure D_2O, suggesting that there is adsorbed material present (Supporting Information). For these films the position of the peak did not change during the loss of mesoscale order.

No diffraction is reported for the C_{14}TAB long PEI conc 1, 1/2, and 1/4 films as these films exhibited macroscopic roughening (buckling) of the surface when the films were grown in the Teflon troughs used for the reflectometry experiments. The origin of this roughening appears to be associated particularly with defects in the Teflon surface (such as small scratches), with the

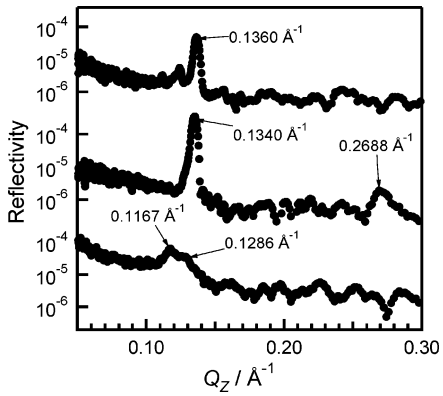

Figure 8. Neutron reflectometry profiles of C_{16}TAB short PEI conc 1 films with different concentrations of NaOH. Top to bottom: 0.100 M NaOH, 0.050 M NaOH, and 0.010 M NaOH.

observed buckles in the film fanning out from these points. If no "nucleation sites" were present in the Teflon surface, then an evenly distributed array of buckles, running perpendicular to the Teflon surface, formed. It is possible that the hydrophobicity of the Teflon facilitates nucleation of the high conc C_{14}TAB films.

In the previous section on BAM, two surface structures were observed during formation of films at certain solutions concentrations. One of the structures present in the C_{16}TAB short PEI conc 1 and 1/2 and the C_{14}-TAB short PEI conc 1/2 films was identified as being fractal in nature. For the C_{16}TAB systems a nonfractal structure was also observed. The neutron reflectometry profiles of these C_{16}TAB films also shows the presence of two structures, and it seems likely that these overlapping diffraction peaks correspond to diffraction from the fractal structure and the nonfractal structures observed in these films. For the C_{14}TAB short PEI conc 1/2 film there is no second structure visible in the BAM images, and only one diffraction peak is observed.

In an expansion of the previously reported experiment, a series of C_{16}TAB short PEI conc 1 films with varying concentrations of NaOH were examined using neutron reflectometry (Figure 8).[25] At low concentrations of hydroxyl ions ($\leq$0.01 M) there is small increase in the peak position, though there is no significant change in the intensity of the diffraction peaks. When the concentration was increased above 0.01 M, there was a significant increase in the intensity of the main diffraction peak, along with further increases in the peak position (decreases in the size of the mesostructure).

From the diffraction peaks observed in the neutron scattering curves, it is possible use the Scherrer formula to determine the size of the crystallites giving rise to the diffraction peak. For both the 0.100 and 0.050 M NaOH containing C_{16}TAB short PEI conc 1 films the size of the crystallites was $\sim$3000 Å. This is much greater than the size of the crystallites in the C_{16}TAB short PEI conc 1/16 film (the most ordered of the non-NaOH containing films), which was calculated to be $\sim$1000 Å.

The swamping of the fractal structure by a large slow forming structure seen in the BAM images indicates that the diffraction peak observed in the 0.05 M NaOH film is derived from this nonfractal structure. Therefore, given the trend in peak positions for the films with added NaOH and the asymmetry of the diffraction peaks on the lower Q_Z side the peak, it is likely that the lower Q_Z peak of two seen in the reflectometry

profile of C_{16}TAB short PEI conc 1, 3/4, and 1/2 films corresponds to the fractal structure. It is probable that the large slow forming structure is an extension of the second structure observed in the NaOH-free systems; however, the BAM images are inconclusive on this point.

Analogous neutron reflectometry experiments (C_{12}TAB and C_{14}TAB short PEI conc 1 and 1/2) using deuterated surfactant and ACMW showed only a slight decrease in the mesostructure size and little change in the peak shape upon substitution of the solvent and surfactant. These changes were not considered significant enough to warrant different interpretations being applied to data collected with D_2O/H_2O as the solvent.

Discussion

From the SANS data it is evident that the formation of the large-scale mesostructures occurs almost exclusively at the interface, as there are no diffraction peaks observed in the SANS profiles and the shape of the micelles in the solution is elliptical rather than rod shaped. The presence of elliptical micelles in solution also shows that there is an association between the polymer and surfactant in solution as nonassociated C_nTAB micelles are close to spherical in shape at the concentration used in these experiments.[46] This result is supported by the experiments of Kudryavtsev and co-workers,[26−28] who used low molecular weight PEI (10 000 and 30 000 Da) and observed that the polymer saturation point (psp) for 0.2 and 0.02 M solutions of PEI occurred at CTAB concentrations of ∼0.008 and 0.006 M. At surfactant concentrations above these, micelles bound to polymer are preferentially formed over less ordered surfactant/polymer aggregates.[14] It is possible that the location of the surfactant and polymer concentrations above the psp are important in the formation of ordered films. The absence of reported films in the work of Kudryavtsev and co-workers may be due to either an absence of a film, perhaps because of the low surfactant and polymer concentrations, or the presence of a thin and therefore less identifiable film. The latter is possible as the molecular weights of the polymers that they used are relatively low, and so any film would probably be quite thin and difficult to visualize with the naked eye. The rate at which the film forms also appears to be dependent on the length of the polymer chain. For long PEI, the BAM and film formation experiments indicate that at high polymer concentration the process takes a number of minutes, whereas for short PEI the BAM images point to a formation time of tens of minutes.

Given the elliptical shape of the micelles in solution the assembly of the film is most likely to occur through the adsorption and rearrangement of these elliptical micelles, along with polymer, at the air/water interface—thereby giving rise to the rodlike micelles observed in the GIXD.[25] Vaknin et al.[13] postulate a related mechanism for the hexagonal structure observed at the interface in their system of oppositely charged surfactant and polyelectrolyte, although in their case they hypothesize that micelle formation is initiated at the interface before occurring in solution, thus leading to micelle encapsulation through sequential adsorption of polyelectrolyte and surfactant to the interface. In that work salt crystallization of the ordered mesostructure was only observed upon addition of salt into the solution. The salt had two roles: to cause the initially ellipsoidal micelles to elongate by binding to the micelle and screening the surface charge and to enhance polyelectrolyte binding to the micelles through entropically favorable counterion release. The elongation of the micelles and the enhanced polymer binding resulted in the ordered mesostructure. In our system, although interactions between the polyelectrolyte and micelles do cause some elongation in the bulk solution, rodlike micelles are also found only at the interface. Addition of salt, however, prevents film formation rather than enhancing it, [25] suggesting a different mechanism operates in this case than in the case of the oppositely charged polymer and surfactant solution. Enhancing polymer binding to the micelle by reducing the charge on the polymer does improve the ordering of micelles within the films possibly because the charged micelles are forced closer together and so pack in a hexagonal array to minimize the electrostatic interaction between adjacent micelles.

The transition to rod-shaped micelles can be considered to be the result of the high local surfactant and counterion concentration at the surface. (In solution the sphere−rod transition occurs when the concentration of surfactant and counterion is increased.[47]) This behavior is very similar to that observed in C_{16}TAB templated silica films, and it is seems reasonable to suggest that the mechanisms for film formation are closely related.[25] However, where the structure of the silica films is stable with time due to the rigidity of the polymerized silica matrix, the necessity for the vessel in which the film is formed to be open to the atmosphere suggests that the formation of the mesostructure in the C_nTAB/PEI systems is kinetically but not thermodynamically favored. If the liquid/vapor equilibrium is established, then the film does not form.

The calculations reported in the film formation section showed that the amount of solid material present in the film was insufficient to allow for all of the film to consist of a highly ordered polymer/surfactant mesostructure. The most likely explanation is that there is a thinner (up to 3 μm thick) layer at the surface, which consists of the ordered mesostructure, below which lies a substantially thicker (up to 100 μm thick) layer of, most likely semiordered, gel phase. This is consistent with the need for evaporation in the film formation process.

A peculiar feature of some of these films is the loss of intensity from the neutron reflectometry profiles with time. There are two possible explanations for this behavior. The first follows from the observation that these films are not thermodynamically favored; that is, the observed decrease in the intensity is caused by dissolution of the film away from the interface. The reason this disordering is observed in the reflectometry profiles of the short PEI but not long PEI films may be related to the smaller thickness of these films and the smaller molecular weight of the polymer. Because of its smaller molecular weight, short PEI will have a reduced number of hydrogen bonds and degree of entanglement and will therefore be able to assemble/dissemble much quicker than long PEI; coupling this with the smaller film thickness, one would expect that dissolution would be much faster in the short PEI systems.

The second possible explanation is that there is an increased ordering of the film that leads to a loss of intensity from peaks from the reflectometry profile. In reflectometry only a small section of the whole diffraction pattern is sampled, and it is assumed either that the sample consists of many crystallites oriented in a

random fashion (effectively a powder diffraction pattern) or that the crystallites, if oriented relative to one another, are oriented in such a way that some of their diffraction spots lie along the $Q_{XY} = 0$ line. However, it is possible that a sample may be highly ordered yet give no diffraction peaks in the reflectometry profile.[48] It may well be the case that the samples in which the diffraction peaks disappear are in fact becoming more ordered with time, rather than less ordered. Paradoxically, this may also be supported by the increased ability of short PEI to assemble itself, as a reduction in the number of entanglements will also lead to a faster rearrangement. A second feature that supports this possibility is the peak shape observed in Figure 7; despite losing intensity, the full width half-maximum of the peak does not appear to change, suggesting that the crystallite size is not decreasing.

In the near future we hope to perform grazing incidence diffraction experiments on these films, the data from which will allow us to determine the correct mechanism.

The variations in the properties of the film with pH indicate that the dominant interaction between the polymer and surfactant is a neutral/cationic interaction, where the dipole on the polymer amine groups interacts with the charged CTAB ammonium groups. However, by increasing the charge on the polymer, it is possible to influence the structure of the films. When the pH is increased (decreasing the net charge on the polymer), there is a shrinking of the size of the mesostructure, i.e., a reduction of the distance between centers of adjacent micelles. These can be attributed to the decreasing level of repulsion between the polymer and surfactant upon loss of the polymers charge, along with the corresponding increase in the number of attractive interactions between the two species. The apparent increase observed in the thickness of the films upon addition of NaOH can also be related to the decreased charge of the polymer, as this will reduce the hydrophilicity of the film, enhancing its surface activity. However, while the level of overall level of structure and ordering is increased, there is a loss of the unique fractal structures from those films that had them at the natural pH, upon reduction of the polymer charge.

The expansion of the mesostructure brought about by increasing the level of protonation in the polymer is also evident in the decrease in the position of the diffraction peak with decreasing polymer concentration. As determined by the pH measurements, the percentage of charged ammonium groups on the polymer increases as the PEI concentration decreases, and this will lead to an increase in the spacing between repeat units in the mesostructure through charge repulsion. A secondary effect of increasing the mesostructure spacing, and therefore decreasing both the density of the film and the level of entanglement and interaction between polymer chains, will be to increase the rate at which the polymer and surfactant can dissociate from each other and rearrange. This effect is manifested by tendency for the lower concentration films to lose their structure faster than the higher concentration films.

A small expansion of the mesostructure may also occur as a result of the uncoiling of the polymer chain due to protonation.[37]

Conclusion

Thin films of PEI and C_nTAB were produced at the air/water interface by mixing solutions of the two components under alkaline conditions. Predominantly these films were highly ordered, containing a hexagonal array of rodlike micelles, running parallel to the air/solution interface, encased in polymer. However, for some of the films, particularly for those prepared with short PEI, this structure disappeared over time, suggesting one of two possibilities: disordering of the film or an enhanced ordering of the film in such a way as to eliminate diffraction peaks from reflectometry profiles.

It was observed that film formation only occurs when the vessels in which the films are formed are not covered (i.e., the solution and vapor are not permitted to equilibrate); thus, the formation of these films is kinetically but not thermodynamically favored.

In these films the main attractive interaction between the polymer and surfactant is a dipole−cation interaction. However, by altering the charge of the polymer, it is possibly to alter the properties of the mesostructure formed, principally the mesostructure spacing.

Acknowledgment. We thank Dr. S. Holt, Dr. R. Dalgliesh, Dr. S. M. King, and Mr. R. Wilson for assistance with the neutron experiments on SURF, CRISP, and LOQ, ISIS. This work, as part of the European Science Foundation EUROCORES Programme SONS, was supported by funds from the EPSRC (GR/S84712/01), the CEA, and the EC Sixth Framework Programme. K.J.E. thanks the Royal Society for a Dorothy Hodgkin Research Fellowship which funded the early part of this work.

Supporting Information Available: A more extensive sample of the BAM images, including those showing the effects of covering the solution; the pH titration curves, samples of the SANS profiles with fits, the lengths and widths of the micelles for all the systems examined, and the fits and scattering length density profiles of the neutron reflectometry profiles modeled using the Parratt program. This material is available free of charge via the Internet at http://pubs.acs.org.

References and Notes

(1) Versic, R. J. In *Flavor Encapsulation*; Risch, S. J., Reineccius, G. A., Eds.; American Chemical Society: Washington, DC, 1988; Vol. 370, pp 126−131.
(2) Simberg, D.; Danino, D.; Talmon, Y.; Minsky, A.; Ferrari, M. E.; Wheeler, C. J.; Barenholz, Y. *J. Biol. Chem.* **2001**, *276*, 47453−47459.
(3) Kötz, J.; Kosmella, S.; Bein, T. *Prog. Polym. Sci.* **2001**, *26*, 1199−1232.
(4) Thünemann, A. F.; Müller, M.; Dautzenberg, H.; Joanny, J.-F.; Löwen, H. In *Polyelectrolytes with Defined Molecular Architectures II*; Springer-Verlag: Berlin, Heidelberg, 2004; Vol. 166, pp 113−171.
(5) Zhou, S. Q.; Chu, B. *Adv. Mater.* **2000**, *12*, 545−556.
(6) Langevin, D. *Adv. Colloid Interface Sci.* **2001**, *89*, 467−484.
(7) Goddard, E. D. *J. Colloid Interface Sci.* **2002**, *256*, 228−235.
(8) Ghosh, K. K.; Sharma, P. *Colloids Surf. A: Physiochem. Eng. Aspects* **2003**, *231*, 113−121.
(9) Folmer, B. M.; Kronberg, B. *Langmuir* **2000**, *16*, 5987−5992.
(10) Penfold, J.; Taylor, D. J. F.; Thomas, R. K.; Tucker, I.; Thompson, L. J. *Langmuir* **2003**, *19*, 7740−7745.
(11) Asnacios, A.; Langevin, A.; Argillier, J. F. *Macromolecules* **1996**, *29*, 7412−7417.
(12) Monteux, C.; Llauro, M.-F.; Baigl, D.; Williams, C. E.; Anthony, O.; Bergeron, V. *Langmuir* **2004**, *20*, 5358−5366.
(13) Vaknin, D.; Dahlke, S.; Travesset, A.; Nizri, G.; Magdazzi, S. *Phys. Rev. Lett.* **2004**, *93*, 218302.
(14) Bystryak, S. M.; Winnik, M. A.; Siddiqui, J. *Langmuir* **1999**, *15*, 3748−3751.
(15) Ray, B.; El Hasri, S.; Guenet, J. M. *Eur. Phys. J. E* **2003**, *11*, 315−323.
(16) Zhou, S.; Burger, C.; Yeh, F.; Chu, B. *Macromolecules* **1998**, *31*, 8157−8163.

(17) Wang, C.; Tam, K. C. *J. Phys. Chem. B* **2004**, *108*, 8976−8982.
(18) Wang, Y. L.; Kimura, K.; Dubin, P. L.; Jaeger, W. *Macromolecules* **2000**, *33*, 3324−3331.
(19) Bromberg, L.; Temchenko, M.; Colby, R. H. *Langmuir* **2000**, *16*, 2609−2614.
(20) Cooke, D. J.; Dong, C. C.; Lu, J. R.; Thomas, R. K.; Simister, E. A.; Penfold, J. *J. Phys. Chem. B* **1998**, *102*, 4912−4917.
(21) Gole, A.; Phadtare, S.; Sastry, M.; Langevin, D. *Langmuir* **2003**, *19*, 9321−9327.
(22) Thünemann, A. F.; Bayermann, J. *Macromolecules* **2000**, *33*, 6878−6885.
(23) Decher, G. *Science* **1997**, *277*, 1232−1237.
(24) Clark, S. L.; Hammond, P. T. *Langmuir* **2000**, *16*, 10206−10214.
(25) Edler, K. J.; Goldar, A.; Brennan, T.; Roser, S. J. *Chem. Commun.* **2003**, 1724−1725.
(26) Zakharova, L. Y.; Valeeva, F. G.; Kudryavtsev, D. B.; Ibragimova, A. R.; Kudryavtseva, L. A.; Timosheva, A. P.; Kataev, V. E. *Kinet. Catal.* **2003**, *44*, 547−551.
(27) Kudryavtsev, D. B.; Bakeeva, R. F.; Kudryavtseva, L. A.; Zakharova, L. Y.; Sopin, V. F. *Russ. Chem. Bull., Int. Ed.* **2000**, *49*, 1501−1505.
(28) Bakeeva, R.; Kudryavtsev, D.; Zakharova, L.; Kudryavtseva, L.; Raevska, A.; Sopin, V. *Mol. Cryst. Liq. Cryst.* **2001**, *367*, 585−596.
(29) Li, Y.; Ghoreishi, S. M.; Warr, J.; Bloor, D. M.; Holzwarth, J. F.; Wyn-Jones, E. *Langmuir* **2000**, *16*, 3093−3100.
(30) Monteux, C.; Williams, C. E.; Bergeron, V. *Langmuir* **2004**, *20*, 5367−5374.
(31) McLoughlin, D.; Langevin, D. *Colloids Surf. A: Physicochem. Eng. Aspects* **2004**, *250*, 79−87.
(32) Penfold, J.; Richardson, R. M.; Zarbakhsh, A.; Webster, J. R. P.; Bucknall, D. G.; Rennie, A. R.; Jones, R. A. L.; Cosgrove, T.; Thomas, R. K.; Higgins, J. S.; Fletcher, P. D. I.; Dickinson, E.; Roser, S. J.; McLure, I. A.; Hillman, A. R.; Richards, R. W.; Staples, E. J.; Burgess, A. N.; Simister, E. A.; White, J. W. *J. Chem. Soc., Faraday Trans.* **1997**, *93*, 3899−3917.
(33) Penfold, J. *Prog. Colloid Polym. Sci.* **1990**, *81*, 198.
(34) Heenan, R. K.; Penfold, J.; King, S. M. *J. Appl. Crystallogr.* **1997**, *30*, 1140−1147.
(35) Parratt, L. G. *Phys. Rev.* **1954**, *95*, 359−369.
(36) Hayter, J. B.; Penfold, J. *Mol. Phys.* **1981**, *42*, 109−118.
(37) Hostetler, R. E.; Swanson, J. W. *J. Polym. Sci.* **1974**, *12*, 29−43.
(38) Moulik, S. P.; Haque, M. E.; Jana, P. K.; Das, A. R. *J. Phys. Chem.* **1996**, *100*, 701−708.
(39) Larsen, J. W.; Magid, L. J. *J. Am. Chem. Soc.* **1974**, *96*, 5774−5782.
(40) Velegol, S. B.; Tilton, R. D. *J. Colloid Interface Sci.* **2002**, *249*, 282−289.
(41) Berr, S. S. *J. Phys. Chem.* **1987**, *91*, 4760−4765.
(42) Quirion, F.; Magid, L. J. *J. Phys. Chem.* **1986**, *90*, 5435−5441.
(43) Ekwall, P.; Mandell, L.; Fontell, K. *J. Colloid Interface Sci.* **1969**, *29*, 639−646.
(44) Eckold, G.; Gorski, N. *Colloids Surf. A: Physiochem. Eng. Aspects* **2001**, *183−185*, 361−369.
(45) Bergström, M.; Pedersen, J. S. *Langmuir* **1998**, *14*, 3754−3761.
(46) Berr, S.; Jones, R. R. M.; Johnson, J. S. *J. Phys. Chem.* **1992**, *96*, 5611−5614.
(47) Nguyen, D.; Bertrand, G. L. *J. Colloid Interface Sci.* **1992**, *150*, 143−157.
(48) Hillhouse, H. W.; van Egmond, J. W.; Tsapatsis, M.; Hanson, J. C.; Larese, J. Z. *Microporous Mesoporous Mater.* **2001**, *44−45*, 639−643.

MA050469K